ELSEVIER

Journal of Power Sources 99 (2001) 78–84

JOURNAL OF POWER SOURCES

www.elsevier.com/locate/jpowsour

Preparation and characterization of high-density spherical $LiNi_{0.8}Co_{0.2}O_2$ cathode material for lithium secondary batteries

Jierong Ying*, Chunrong Wan, Changyin Jiang, Yangxing Li

Institute of Nuclear Energy Technology, Tsinghua University, P.O. Box 1021, Beijing 102201, PR China

Received 9 February 2000; received in revised form 24 May 2000; accepted 20 December 2000

Abstract

The lithium secondary batteries with high power density need the electrode materials with both high specific capacity and high tap-density. $LiNi_{0.8}Co_{0.2}O_2$ cathode material is a very promising candidate to replace the commercialized $LiCoO_2$ for lithium secondary batteries. Spherical $Ni_{0.8}Co_{0.2}(OH)_2$ powders were prepared via a ''controlled crystallization'' method using $NiSO_4$, $CoSO_4$, NaOH and $NH_3{\cdot}H_2O$. Spherical $LiNi_{0.8}Co_{0.2}O_2$ powders with order layered structure were easily synthesized by firing $LiOH{\cdot}H_2O$ and the spherical $Ni_{0.8}Co_{0.2}(OH)_2$ in oxygen at 750°C for 8 h. The relation among the ''controlled crystallization'' conditions and the $Ni_{0.8}Co_{0.2}(OH)_2$ and $LiNi_{0.8}Co_{0.2}O_2$ powders' structure, particle morphology, particle size, particle size distribution, and tap-density was investigated. It is shown that with the suitable ''controlled crystallization'' conditions, the tap-density of the spherical $LiNi_{0.8}Co_{0.2}O_2$ powders can be improved as high as 3.24 g cm^{-3}, which is remarkably higher than the non-spherical $LiNi_{0.8}Co_{0.2}O_2$ powders available as commercial cathode materials. The cathode materials also show high reversible specific capacity and long cycling life. The high-density spherical $LiNi_{0.8}Co_{0.2}O_2$ cathode materials can greatly improve the power density of the lithium secondary batteries.

Keywords: Lithium secondary batteries; ''Controlled crystallization'' method; $LiNi_{0.8}Co_{0.2}O_2$; High-density; Spherical

1. Introduction

The layered $LiNi_{1-x}Co_xO_2$ ($0 < x < 1$) series of compounds have been extensively studied as cathode materials for lithium secondary batteries [1–7]. These materials are considered as strong potential candidates to replace the actually commercialized $LiCoO_2$ because of their attractive advantages, such as lower cost and higher reversible capacity than $LiCoO_2$, easier preparation and better cycling stability than $LiNiO_2$, etc. Among these compounds, $LiNi_{0.8}Co_{0.2}O_2$ appears to be much more promising [1–4].

The power density of the lithium secondary batteries keeps on being improved. For this reason, it is very important and significant to prepare electrode materials with both high specific capacity and high density. However, the electrode pellets are usually manufactured by mixing electrode material powders, electroconductive materials, binders, and fillers, etc. The practical density of the electrode materials in the pellets is not only due to the materials' theoretical density, but also due to a lot of other factors. According to the practice, it has been shown that the higher the tap-density, the higher the practical density is [8]. In other words, the tap-density is consistent with the practical density. Thus, what we should do is to prepare electrode materials with both high specific capacity and high tap-density. Unfortunately, it is well known that the high tap-density brings low specific capacity. In fact, this conclusion is not absolutely correct. The tap-density of the electrode material powders is usually improved by increasing the materials' crystallinity and crystalline grains' size. The decreased specific capacity is mainly due to the higher crystallinity and larger crystalline grains. Actually, the tap-density of the powders is nearly related to the powders' particle morphology, particle size, and particle size distribution, etc. For example, $Ni(OH)_2$ has been widely used as cathode material in the Ni–MH rechargeable batteries. The tap-density of the sheet $Ni(OH)_2$ powders is as low as 1.5–1.6 g cm^{-3}. In comparison, the tap-density of the spherical $Ni(OH)_2$ powders without increasing the crystallinity and lowering the specific capacity is as high as 2.1–2.2 g cm^{-3} [8]. The power density of the Ni–MH rechargeable batteries using the spherical $Ni(OH)_2$ cathode material has been greatly improved. According to the fact, we can expect that the electrode materials with both high specific capacity and

* Corresponding author. Tel.: +86-10-62773274; fax: +86-10-69771464.
E-mail addresses: yjr99@263.net, yjr99@yahoo.com.cn (J. Ying).

0378-7753/01/$ – see front matter
PII: S0378-7753(01)00477-3

high tap-density are sure to be prepared by controlling the powders' particle morphology, particle size, and particle size distribution. It is expected that preparing spherical powders may be an effective way.

The theoretical density of $LiNi_{0.8}Co_{0.2}O_2$ is about 4.78 g cm^{-3}. However, the tap-density of the commercialized $LiNi_{0.8}Co_{0.2}O_2$ powders is usually as low as 2.3 g cm^{-3}. The commercialized $LiNi_{0.8}Co_{0.2}O_2$ powders are usually prepared via conventional solid state reaction of lithium compounds, nickel compounds and cobalt compounds [2]. The obtained $LiNi_{0.8}Co_{0.2}O_2$ powders always show irregular particle morphology with broad particle size distribution. These disadvantages result in the low tap-density. In our laboratory, the spherical $Ni(OH)_2$ powders with different particle morphology, particle size, particle size distribution, and tap-density have been prepared via a ''controlled crystallization'' method using $NiSO_4$, $CoSO_4$, NaOH and $NH_3{\cdot}H_2O$ [8]. The products have been widely used in the Ni–MH rechargeable batteries. Since the crystal structure and solubility products of $Ni(OH)_2$ and $Co(OH)_2$ are very similar, it is possible to synthesize spherical $Ni_{0.8}Co_{0.2}(OH)_2$ with a very homogeneous distribution of Ni^{2+} and Co^{2+} on the atomic scale via the ''controlled crystallization'' method. And then, the spherical $LiNi_{0.8}Co_{0.2}O_2$ with a very homogeneous distribution of Ni^{3+} and Co^{3+} on the atomic scale can be prepared by sintering the spherical $Ni_{0.8}Co_{0.2}(OH)_2$ mixed with certain lithium compound, such as $LiOH{\cdot}H_2O$. The particle morphology, particle size, particle size distribution, and tap-density of the $LiNi_{0.8}Co_{0.2}O_2$ powders can be controlled by adjusting the ''controlled crystallization'' conditions. The above results have scarcely been reported so far.

In this paper, the preparation, structure and electrochemical performance of the spherical $LiNi_{0.8}Co_{0.2}O_2$ powders with high tap-density and high specific capacity have been discussed in detail.

2. Experimental

Referring to the ''controlled crystallization'' methods of preparing spherical $Ni(OH)_2$ described in reference [8–11], the spherical $Ni_{0.8}Co_{0.2}(OH)_2$ was synthesized as the follows. The solution of $NiSO_4$ and $CoSO_4$ (Ni/Co = 4.0, molar ratio) was pumped continuously into a special reactor. At the same time, the solution of NaOH and $NH_3{\cdot}H_2O$ (acts as chelating agent) was also pumped into the reactor. $Ni_{0.8}Co_{0.2}(OH)_2$ was obtained according to the reaction:

$$0.8NiSO_4 + 0.2CoSO_4 + 2NaOH = Ni_{0.8}Co_{0.2}(OH)_2 \downarrow + Na_2SO_4$$

The concentration of the two solutions, average rest time (or the feed-in velocity), agitating intensity, temperature, pH, and total concentration of ammonia (C_{NH_3}) of the mixture being agitating vigorously in the reactor should be controlled carefully. Thus, the crystallization and growth of $Ni_{0.8}Co_{0.2}(OH)_2$ particles in the reactor could be controlled effectively. The irregular particles changed gradually into spherical particles after enough time of reaction and agitation. The mixture in the reactor was filtered, washed and dried. Thus, the spherical $Ni_{0.8}Co_{0.2}(OH)_2$ powders were obtained. According to the result of preparing spherical $Ni(OH)_2$ by the ''controlled crystallization'' method, the pH and C_{NH_3} of the mixture are the most important factors to affect the powders' crystal structure, particle morphology, particle size, and particle size distribution. In this work, five samples of $Ni_{0.8}Co_{0.2}(OH)_2$ powders were prepared with different pH and C_{NH_3}, as listed in Table 1. Other ''controlled crystallization'' parameters were as follows: the total concentration of the $NiSO_4/CoSO_4$ solution was 2.0 mol l^{-1}. The concentration of the NaOH solution was 5.0 mol l^{-1}. The agitating intensity was 50 W l^{-1}. The average rest time was 10 h. The temperature was 60°C. The spherical $Ni_{0.8}Co_{0.2}(OH)_2$ and $LiOH{\cdot}H_2O$ powders, in a molar ratio of Li:(Ni + Co) = 1.02:1.00, were mixed uniformly. The mixed powders were sintered at 750°C for 8 h in oxygen to obtain spherical $LiNi_{0.8}Co_{0.2}O_2$ powders. The five samples of $LiNi_{0.8}Co_{0.2}O_2$ powders are listed in Table 1 corresponding to the five samples of $Ni_{0.8}Co_{0.2}(OH)_2$ precursors.

Table 1
The samples of $Ni_{0.8}Co_{0.2}(OH)_2$ and $LiNi_{0.8}Co_{0.2}O_2$ and the corresponding ''controlled crystallization'' parameters of pH and C_{NH_3}

Sample name of the $Ni_{0.8}Co_{0.2}(OH)_2$ powders	Sample name of the $LiNi_{0.8}Co_{0.2}O_2$ powders	pH	C_{NH_3} (mol l^{-1})
N1	L1	9.5	0.3
N2	L2	10.5	0.3
N3	L3	11.5	0.3
N4	L4	12.5	0.3
N5	L5	11.5	0.6

The metal elements molar ratio of the powders was evaluated by inductively coupled plasma (ICP) emission spectroscopy. Powder X-ray diffraction (XRD, D/max-rB) using Cu Kα radiation was used to identify the crystalline phase and crystal lattice parameters of the powders. The particle morphology, particle size and particle size distribution of the powders were observed using a scanning electron microscopy (SEM, JSM6301F). The tap-density of the powders was tested using the method described in reference [11].

Experimental test cells for measurements used the cathode with the composition of 80 wt.% $LiNi_{0.8}Co_{0.2}O_2$, 10 wt.% carbon black, and 10 wt.% PTFE. The separator was a Celguard 2400 microporous polylene membrane. The electrolyte was 1 M $LiPF_6$ EC + DEC (1:1 by volume). A lithium metal anode was used in this study. The cells were assembled in a glove box filled with argon gas. The charge–discharge cycling was galvanostatically performed at a current density of 0.5 mA cm^{-2} with cut-off voltages of 3.0–4.3 V (versus Li/Li^+) at 20°C.

The structure and performance of the non-spherical $LiNi_{0.8}Co_{0.2}O_2$ powders obtained from Merck were discussed in comparison with the spherical $LiNi_{0.8}Co_{0.2}O_2$ powders prepared in this work.

3. Results and discussion

The molar ratio of Ni:Co of each of the five samples of $Ni_{0.8}Co_{0.2}(OH)_2$ powders was determined through ICP analysis. The result is exactly the same as the designed value which is Ni:Co = 4.0:1.0. It is proved that with the suitable ''controlled crystallization'' conditions, $Ni(OH)_2$ and $Co(OH)_2$ can be actually coprecipitated homogeneously.

Fig. 1 shows the morphology of the $Ni_{0.8}Co_{0.2}(OH)_2$ powders of N1, N2, N3, N4, and N5. Fig. 1(N1(a)) shows the particles of N1 are spherical with the particle size of about 3–20 μm. Each of the spherical particles is made up of a large number of fine crystalline grains, which are piling loosely to form netlike structure, as shown in Fig. 1(N1(b)).

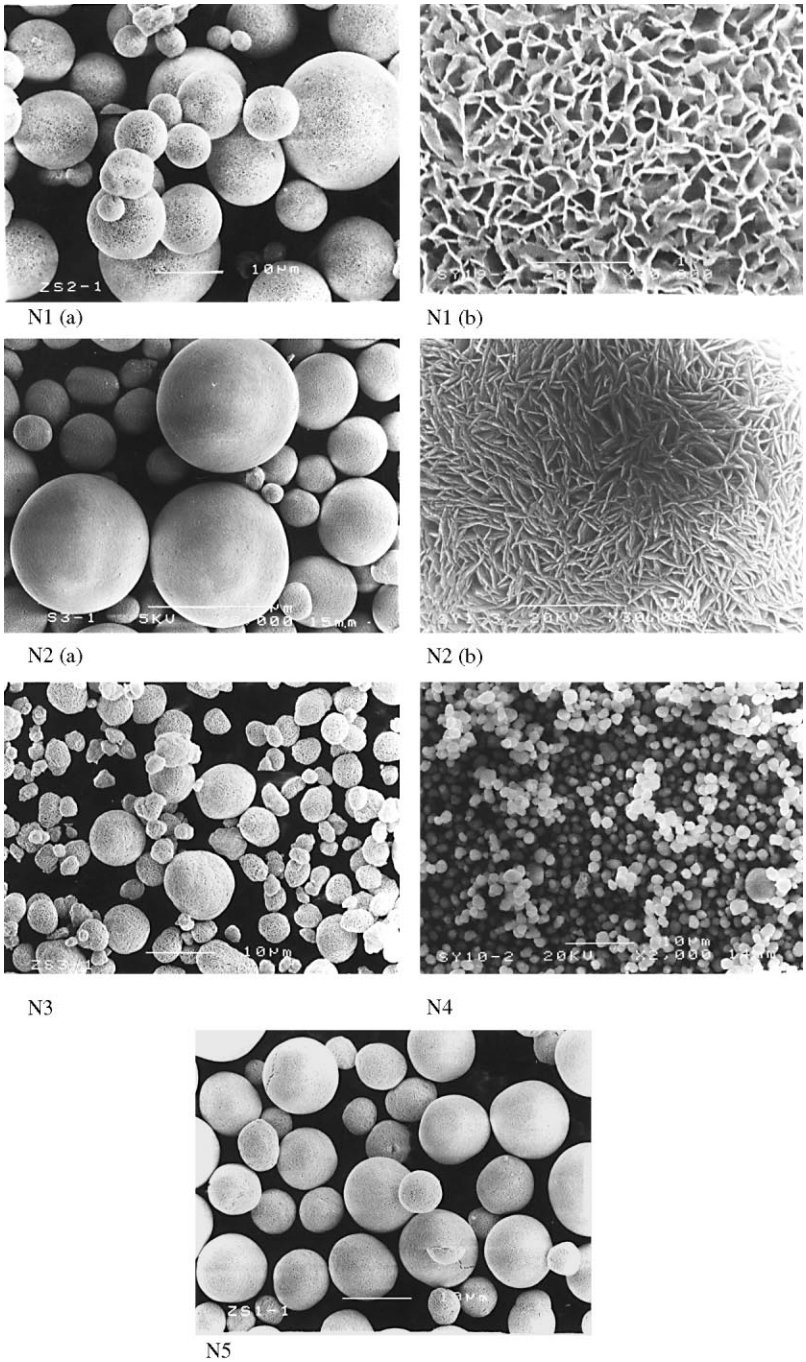

Fig. 1. SEM images of the $Ni_{0.8}Co_{0.2}(OH)_2$ prepared by ''controlled crystallization'' method.

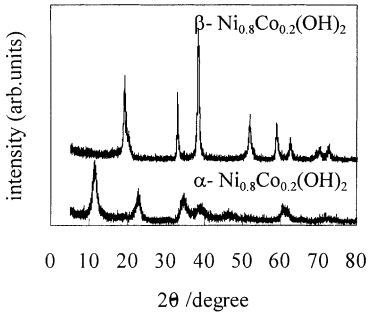

Fig. 2. X-ray diffraction pattern of the $Ni_{0.8}Co_{0.2}(OH)_2$ powders.

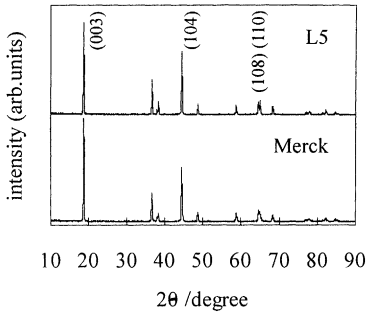

Fig. 3. X-ray diffraction pattern of the $LiNi_{0.8}Co_{0.2}O_2$ powders.

The underside of Fig. 2 shows the XRD spectra of N1. It can be observed that the spectra is almost the same as the spectra of pure α-$Ni(OH)_2$. The absence of any other signals indicates that the Co^{2+} is homogeneously distributed within the NiO_2 layers of $Ni(OH)_2$. The crystal lattice parameters of the layered α-$Ni_{0.8}Co_{0.2}(OH)_2$ are $a = 3.0487$ Å and $c = 23.4226$ Å. The interlayer distance is as high as 7.8075 Å (c/3). It is tested that the tap-density of N1 is only 0.52 g cm^{-3} because of the loose structure and large interlayer distance.

As the pH being increased to 10.5 from 9.5, the particle size and particle size distribution of N2 are similar with that of N1, as shown in Fig. 1(N2(a)). However, each of the spherical particles of N2 is made up of a large number of fine club-shaped crystalline grains, which are piling closely, as shown in Fig. 1(N2(b)). The upside of Fig. 2 shows the XRD spectra of N2 is very different from that of N1. The spectra of N2 is almost the same as the spectra of pure β-$Ni(OH)_2$. The crystal lattice parameters of the layered β-$Ni_{0.8}Co_{0.2}(OH)_2$ are $a = 3.1175$ Å and $c = 4.6086$ Å. The interlayer distance is as low as 4.6086 Å (c). It is tested that the tap-density of N2 is as high as 2.16 g cm^{-3} because of the close structure and small interlayer distance.

As the pH being further increased to 11.5 and 12.5 from 10.5, the piling structure of crystalline grains, the XRD spectra and the crystal lattice parameters of N3 and N4 are similar to that of N2. However, when pH is higher than 10.5, the pH will affect the powders' particle morphology, particle size, and particle size distribution obviously. As indicated in Fig. 1(N2(a), N3 and N4), the average particle size of the powders is decreasing while the pH is increasing. In comparison with N1 and N2, the shape of the particles of N3 and N4 becomes quasi-spherical. As a result, the tap-density of N3 and N4 is only 2.08 and 1.88 g cm^{-3}, respectively.

The samples of N1, N2, N3, and N4 are prepared with the same C_{NH_3} of 0.3 mol l^{-1}. The sample of N5 is prepared with the C_{NH_3} of 0.6 mol l^{-1} and pH of 11.5. It is found the piling structure of crystalline grains, the XRD spectra and the crystal lattice parameters of N5 are similar to that of N2, N3, and N4. As shown in Fig. 1(N5), the shape of the particles of N5 becomes much more spherical than that of N3. In comparison with N1 and N2, the particle size distribution of N5 is much narrower. Most of the particles have the size of 5–15 μm. The perfect spherical particles and narrow particle size distribution result in the high tap-density of 2.25 g cm^{-3}, which is higher than that of N1, N2, N3, and N4.

The $Ni_{0.8}Co_{0.2}(OH)_2$ powders of N1, N2, N3, N4, and N5 were homogeneously mixed with $LiOH{\cdot}H_2O$ and sintered at 750°C for 8 h in oxygen to synthesize $LiNi_{0.8}Co_{0.2}O_2$ powders of L1, L2, L3, L4 and L5, respectively. The ICP analysis shows the molar ratios of Li:Ni:Co of L5 and the Merck's $LiNi_{0.8}Co_{0.2}O_2$ are 0.994:0.802:0.198 and 0.994:0.798:0.202, respectively. The ICP analysis also shows there is negligible difference among the composition of L1, L2, L3, L4 and L5. The X-ray diffraction patterns of L5 and the Merck's $LiNi_{0.8}Co_{0.2}O_2$ are shown in Fig. 3. The spectra of L5 is very similar to that of Merck's $LiNi_{0.8}Co_{0.2}O_2$. The materials calcined at 750°C for 8 h are well crystallized into phase-pure $LiNi_{0.8}Co_{0.2}O_2$ powders without any development of minor phases. The spectra also shows a large integrated intensity ratio $I(0\ 0\ 3)/I(1\ 0\ 4) = 1.43$ and a clear split of the (1 0 8) and (1 1 0) peaks which are indicative of less disorder in the structure. The crystal lattice parameters of the layered $LiNi_{0.8}Co_{0.2}O_2$ are $a = 2.8583$ Å and $c = 14.1496$ Å, which are slightly larger than that of the Merck's one ($a = 2.8553$ Å and $c = 14.1180$ Å). The XRD analysis shows there is negligible difference among the crystalline phase and crystal lattice parameters of L1, L2, L3, L4 and L5.

In contrast to the negligible difference of composition, crystalline phase and crystal lattice parameters among L1, L2, L3, L4 and L5, there is obvious difference of particle morphology, particle size, particle size distribution, and tap-density among the five samples and the Merck's $LiNi_{0.8}Co_{0.2}O_2$. Figs. 4 and 5 show the morphology of the $LiNi_{0.8}Co_{0.2}O_2$ powders of L1, L2, L3, L4, L5 and the Merck's one. As can be found in Fig. 4(L1(a)), the spherical particles of L1 shrank after sintering because of the loose structure of N1. The particle size of L1 is about 3–10 μm. Fig. 4(L1(b)) shows the crystal grains of L1 are larger and piling more closely than that of N1, but there are still a lot of interspace within the spherical particles. The particle morphology, particle size, particle size distribution of L2, L3, L4, and L5 are almost the same as their precursors of N2, N3, N4, and N5, respectively. The structure of the spherical particles

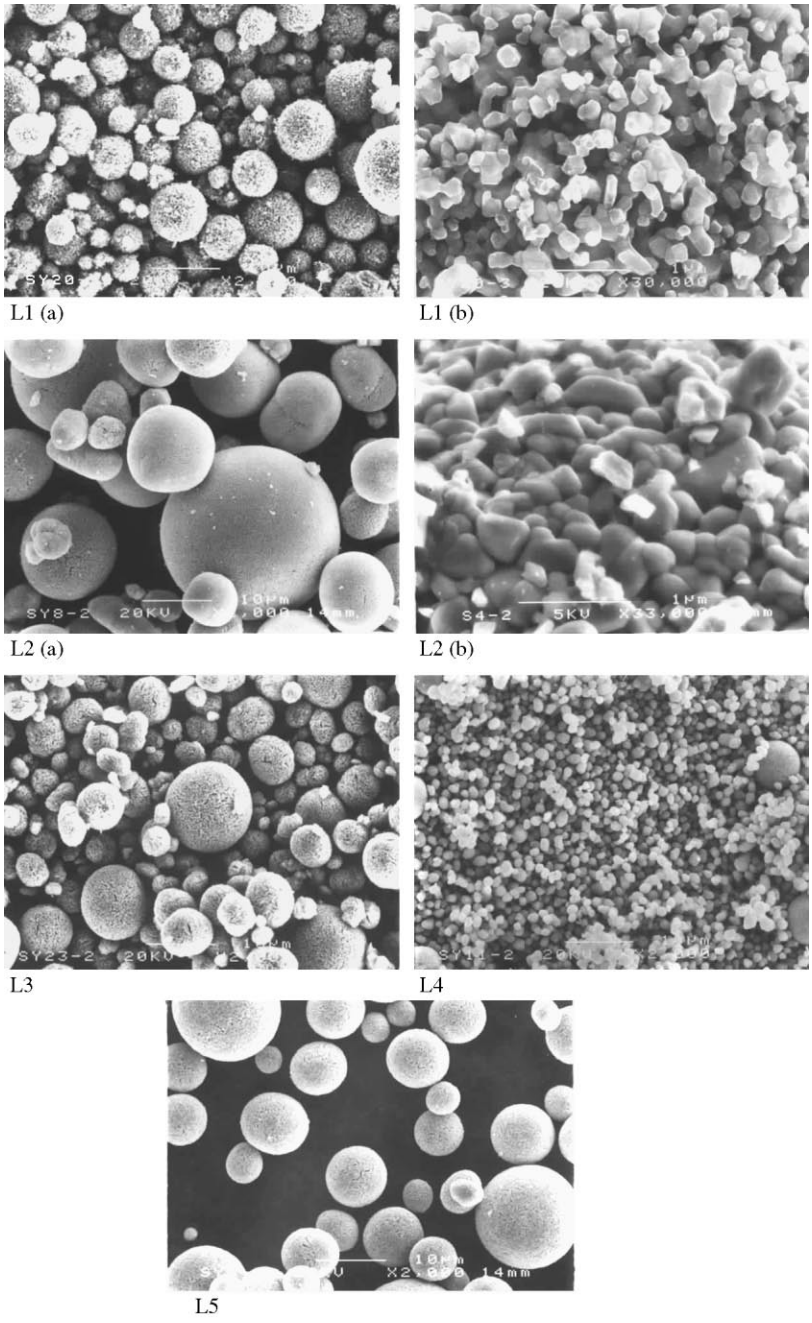

Fig. 4. SEM images of the spherical $LiNi_{0.8}Co_{0.2}O_2$ prepared in this work.

of L3, L4, and L5 is similar to that of L2, as shown in Fig. 4(L2(b)). Each of the spherical particles is made up of a large number of closely piled granular crystalline grains which are different from the fine club-shaped crystalline grains of the $Ni_{0.8}Co_{0.2}(OH)_2$ particles, indicating that the crystalline grains fused and increased during calcination. Fig. 5 shows the morphology of the Merck's $LiNi_{0.8}Co_{0.2}O_2$ powders. As shown in Fig. 5(a), the Merck's $LiNi_{0.8}Co_{0.2}O_2$ powders are composed of irregular particles with broad particle size distribution. The larger crystalline grains indicate that the material has higher crystallinity than the spherical $LiNi_{0.8}Co_{0.2}O_2$ prepared in this work, as shown in Fig. 5(b). The tap-density of L1, L2, L3, L4, L5, and the Merck's $LiNi_{0.8}Co_{0.2}O_2$ is listed in Table 2 together with N1, N2, N3, N4, and N5.

Accordingly, the Merck's $LiNi_{0.8}Co_{0.2}O_2$ has higher crystallinity than the spherical $LiNi_{0.8}Co_{0.2}O_2$ prepared in this work. It seems as if the former has higher tap-density than the latter. In fact, the tap-density of the Merck's $LiNi_{0.8}Co_{0.2}O_2$ powders is only 2.27 g cm^{-3}, which is lower than that of L1, L2, L3, L4, and L5, as indicated in Table 2. It can be concluded that the particle morphology is a very important factor on the tap-density of the $LiNi_{0.8}Co_{0.2}O_2$ powders. The powders composed of spherical particles have higher

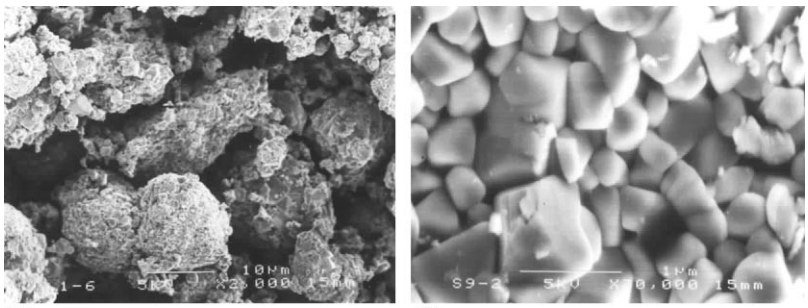

Fig. 5. SEM images of the Merck's $LiNi_{0.8}Co_{0.2}O_2$.

tap-density than the powders composed of irregular particles. The reasons may be as follows. In general, there are serious agglomeration and ''bridge formation'' of particles within the powders composed of irregular particles. The phenomena result in a lot of vacancies among the particles and the bad fluidity of the powders. Therefore, the powders composed of irregular particles are very difficult to be packed closely even after long period of taping. The powders have low tap-density because there is still a lot of space within the powders after long period of taping. In contrast, there are much less agglomeration and ''bridge formation'' of particles within the powders composed of spherical particles because the spherical particles have less contacting interface among each other. The phenomena result in less vacancy among the particles and the excellent fluidity of the powders. The powders composed of spherical particles are easy to be packed closely after taping because of the excellent fluidity. During been taping, the small spherical particles can easily move and occupy the vacancies among the large spherical particles. The spherical powders have high tap-density because there are only a small quantity of space within the powders after long period of taping. Of course, the tap-density of the spherical $LiNi_{0.8}Co_{0.2}O_2$ powders nearly depends on the powders' particle morphology, particle size, particle size distribution, as indicated in Table 2. It is found the smaller the average particle size, the lower the tap-density is. The tap-density of L4 is only 2.41 g cm^{-3} because of the very small average particle size. The tap-density of L5 is larger than L3 because the particles of L5 have better sphericity than L3. The tap-density of L5 is larger than L2 because L5 have narrow and reasonable particle size distribution. The tap-density of L1 is much lower than that of L2 because L1 has loose particle structure. Though the tap-density of the spherical $LiNi_{0.8}Co_{0.2}O_2$ powders is related to a lot of factors, it nearly depends on the tap-density of the corresponding $Ni_{0.8}Co_{0.2}(OH)_2$ precursors, as shown in Table 2. It can be found the higher tap-density the $Ni_{0.8}Co_{0.2}(OH)_2$ precursors, the higher tap-density the $LiNi_{0.8}Co_{0.2}O_2$ powders is. Thus, by adjusting the ''controlled crystallization'' conditions to prepare the spherical $Ni_{0.8}Co_{0.2}(OH)_2$ precursors powders, we can not only control the $LiNi_{0.8}Co_{0.2}O_2$ powders' particle morphology, particle size, particle size distribution, but also control the $LiNi_{0.8}Co_{0.2}O_2$ powders' tap-density. L5 has the highest tap-density among the spherical $LiNi_{0.8}Co_{0.2}O_2$ powders prepared in this work. However, the tap-density is much lower than the theoretical density of $LiNi_{0.8}Co_{0.2}O_2$ which is about 4.78 g cm^{-3}. It is expected that the tap-density of the $LiNi_{0.8}Co_{0.2}O_2$ powders can be further increased by optimizing the particle morphology, particle size, particle size distribution. It can be realized through optimizing the ''controlled crystallization'' conditions to prepare the spherical $Ni_{0.8}Co_{0.2}(OH)_2$ precursors powders.

Table 2
Tap-density of the $Ni_{0.8}Co_{0.2}(OH)_2$ and $LiNi_{0.8}Co_{0.2}O_2$ powders

Sample	Tap-density (g cm^{-3})	Sample	Tap-density (g cm^{-3})
N1	0.52	L1	2.32
N2	2.16	L2	3.08
N3	2.08	L3	2.90
N4	1.88	L4	2.41
N5	2.25	L5	3.24
		$LiNi_{0.8}Co_{0.2}O_2$ (Merck)	2.27

The spherical $LiNi_{0.8}Co_{0.2}O_2$ cathode materials not only have high tap-density, but also have high specific capacity and good cycling stability. We tested the Li/1.0 M $LiPF_6$-EC/DEC/$LiNi_{0.8}Co_{0.2}O_2$ cells using spherical $LiNi_{0.8}Co_{0.2}O_2$ powders of L5 prepared in this work and the Merck's $LiNi_{0.8}Co_{0.2}O_2$ powders. Cycling was carried out galvanostatically at constant charge–discharge current density of 0.5 mA cm^{-2} between 3.0 and 4.3 V at 20°C. As Fig. 6 illustrates, the cathode material of L5 has a first cycle charge

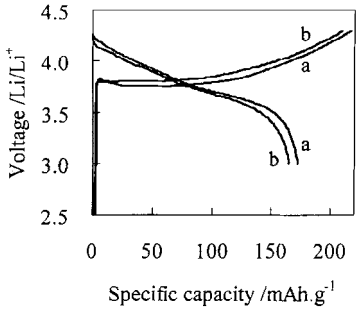

Fig. 6. Charge–discharge curves of the first cycle.

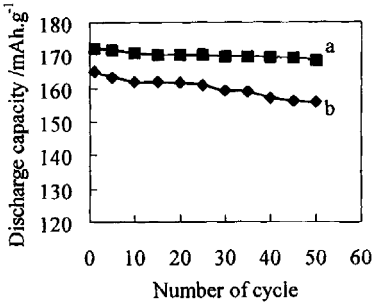

Fig. 7. Variation of specific discharge capacity with number of cycles.

capacity of 217 mAh g^{-1} followed by a discharge capacity of 172 mAh g^{-1}. The coulombic efficiency for the first cycle is 79.3%. However, the $LiNi_{0.8}Co_{0.2}O_2$ powders obtained from Merck Corporation only has a first cycle charge capacity of 210 mAh g^{-1} followed by a discharge capacity of 165 mAh g^{-1} with the coulombic efficiency of 78.5%. Fig. 7 shows the cycle performance of the two kinds of $LiNi_{0.8}Co_{0.2}O_2$ samples. The initial reversible specific capacity of L5 is 172 mAh g^{-1} with a capacity loss of 2.15% in 50 cycles or about 0.04% per cycle, which is obviously improved comparing with the Merck's one. According to the testing, there is negligible difference of reversible specific capacity and cycling stability among L1, L2, L3, L4 and L5.

The high specific reversible capacity and excellent cycling stability of the spherical $LiNi_{0.8}Co_{0.2}O_2$ cathode materials are partly attributed to the advanced preparation. The spherical $Ni_{0.8}Co_{0.2}(OH)_2$ precursors with a very homogeneous distribution of Ni^{2+} and Co^{2+} on the atomic scale can be synthesized via the "controlled crystallization" method. It can therefore ensure a very homogeneous distribution of Ni^{3+} and Co^{3+} on the atomic scale in $LiNi_{0.8}Co_{0.2}O_2$. However, The Merck's $LiNi_{0.8}Co_{0.2}O_2$ powders are prepared via conventional solid state reaction, which is almost impossible to realize the homogeneous distribution of Ni^{3+} and Co^{3+} on the atomic scale. Additional, it is relatively easier to synthesize $LiNi_{0.8}Co_{0.2}O_2$ from $Ni_{0.8}Co_{0.2}(OH)_2$ precursors because the layered structure of $Ni_{0.8}Co_{0.2}(OH)_2$ and $LiNi_{0.8}Co_{0.2}O_2$ is very similar. The order layered structure of $Ni_{0.8}Co_{0.2}(OH)_2$ precursor ensures the ordered layered structure of $LiNi_{0.8}Co_{0.2}O_2$, as has been indicated by the X-ray diffraction patterns. The lower crystallinity and smaller crystalline grains of the spherical $LiNi_{0.8}Co_{0.2}O_2$ may be another reason for the higher specific capacity than Merck's one.

The spherical $LiNi_{0.8}Co_{0.2}O_2$ powders prepared in this work have both high specific capacity and high tap-density. The contradiction between high specific capacity and high tap-density of the materials has been solved satisfactorily. In order to solve the contradiction, we improve the $LiNi_{0.8}Co_{0.2}O_2$ powders' tap-density by controlling the powders' particle morphology, particle size, and particle size distribution, not by increasing the powders' crystallinity and crystalline grains' size. Therefore, the tap-density of the spherical $LiNi_{0.8}Co_{0.2}O_2$ powders hardly affects the cathode materials' specific capacity. Since there is negligible difference of composition, crystalline phase, crystal lattice parameters, and crystallinity among L1, L2, L3, L4 and L5, there is negligible difference of specific capacity among them.

4. Conclusions

The spherical $LiNi_{0.8}Co_{0.2}O_2$ powders with high specific capacity were synthesized in this work. The cathode materials' tap-density was greatly improved. The high-density spherical $LiNi_{0.8}Co_{0.2}O_2$ cathode material is then a very promising candidate to be used in the lithium secondary batteries with high power density.

The particle size, particle size distribution, and tap-density of the spherical $LiNi_{0.8}Co_{0.2}O_2$ powders are closely related to the "controlled crystallization" conditions of synthesizing the spherical $Ni_{0.8}Co_{0.2}(OH)_2$ precursors. The "controlled crystallization" method is the foundation to synthesize high-density spherical $LiNi_{0.8}Co_{0.2}O_2$ cathode materials, and is significant to be further studied.

Acknowledgements

This study is supported by the National Science Foundation of China (Project 50002006) and the Basic Research Foundation of Tsinghua University (Project JC1999054).

References

[1] Y. Li, Applied Chemistry, Ph.D. Thesis, Institute of Nuclear Energy Technology, Tsinghua University, Beijing, PR China, 1999.
[2] Saadoune, C. Delmas, J. Solid State Chem. 136 (1998) 8–15
[3] A.G. Ritchie, C.O. Giwa, J.C. Lee, et al., J. Power Sources 80 (1999) 98–102.
[4] D. Caurant, N. Baffier, B. Carcia, et al., Solid State Ionics 91 (1996) 45–54.
[5] B. Banov, J. Bourilkov, M. Mladenov, J. Power Sources 54 (1995) 268–270.
[6] R. Alcantara, J. Morales, J.L. Tirado, et al., J. Electrochem. Soc. 142 (12) (1995) 3997–4005
[7] R. Alcatara, P. Lavela, J.L. Tirado, et al., J. Electrochem. Soc. 145 (3) (1998) 730–736
[8] C. Jiang, C. Wan, Q. Zhang, et al., Chin. J. Power Sources 21 (6) (1997) 243–247.
[9] C. Zhaorong, L. Gongan, Z. Yujuan, et al., J. Power Sources 74 (1998) 252–254.
[10] Z. Hui, R. Xiaohua, J. Wenquan, et al., Chin. J. Power Sources 23 (Suppl.) (1999) 67–69.
[11] C. Wan, J. Zhang, C. Jiang, Tsinghua Univ. (Sci. Technol.) 38 (5) (1998) 95–98.